[UCI]I804:21031-200000293448

Thesis for the Degree of Master of Engineering

Stochastic Analysis of Rainwater Harvesting System and its Application as Climate Change Adaptation Facility

by

Inkyeong Sim
Division of Earth Environmental System Science
(Major of Environmental Engineering)
The Graduate School
Pukyong National University

February 2020

Stochastic Analysis of Rainwater Harvesting System and its Application as Climate Change Adaptation Facility

(빗물이용시설의 추계학적 해석 및 기후변화 적응시설로서의 활용성 분석)

Advisor: Prof. Sangdan Kim

by

Inkyeong Sim

A thesis submitted in partial fulfillment of the requirements
for the degree of

Master of Engineering

in Division of Earth Environmental System Science
(Major of Environmental Engineering),
The Graduate School, Pukyong National University

February 2020

Stochastic Analysis of Rainwater Harvesting System and its Application as Climate Change Adaptation Facility

A dissertation
by
Inkyeong Sim

Approved by:

(Chairman) Lee, Taeyoon

(Member) Noh, Youngmin

(Member) Kim, Sangdan

February 21, 2020

List of Contents

Ⅰ. **Introduction** ·· 1

1.1. Background ·· 1

1.2. Objectives ·· 2

Ⅱ. **Materials and methods** ·· 6

2.1. Data ·· 6

2.2. EPA SWMM ·· 7

2.3. Stochastic model for dynamic water balance in RHS ·········· 8

2.4. Steady-state PDF for normalized depth of RHS ················· 17

2.5. Water supply reliability and stormwater interception ratio ·· 20

Ⅲ. **Results** ·· 22

3.1. Stochastic model verification ·· 22

3.2. Further analysis of stochastic RHS model ···························· 27

3.2.1. Sensitivity analysis by parameter ·· 27

3.2.2. Sensitivity analysis by parameter combination ················· 33

Ⅳ. **Applications** ·· 38

4.1. Design formula of water supply reliability and stormwater interception ratio ·· 38

4.2. RHS mitigates adverse effects of climate change ··············· 41

Ⅴ. Conclusions ··· 46

References ··· 50

List of Figures

Fig. 2.1 Schematic of inflow into and outflow from a RHS. ························ 9
Fig. 2.2 Probability density function of rainfall depth. ································ 10
Fig. 2.3 Probability density function of inflow. ·· 14
Fig. 2.4 Loss function. ·· 15
Fig. 3.1 Comparisons of water supply reliability R_e in 6 sites. ················· 23
Fig. 3.2 Comparisons of stormwater interception ratio R_r in 6 sites. ········ 24
Fig. 3.3 Water supply reliability and stormwater interception ratio of RHS with varying storage capacities. ··· 25
Fig. 3.4 Water supply reliability and stormwater interception ratio of RHS with varying water demands. ··· 26
Fig. 3.5 Water supply reliability and stormwater interception ratio of RHS with varying roof areas. ·· 26
Fig. 3.6 CDF of s with varying storage capacities. ···································· 28
Fig. 3.7 CDF of s with varying water demands. ·· 29
Fig. 3.8 CDF of s with varying roof areas. ·· 29
Fig. 3.9 Mean of s and p_0 with varying storage capacities. ······················· 31
Fig. 3.10 Mean of s and p_0 with varying water demands. ························ 31
Fig. 3.11 Mean of s and p_0 with varying roof areas. ······························· 32
Fig. 3.12 Water supply reliability R_e varying with storage capacities and water demands. ·· 34
Fig. 3.13 Water supply reliability R_e varying with water demands and roof

areas. ·· 34
Fig. 3.14 Water supply reliability R_e varying with roof areas and storage capacities. ·· 35
Fig. 3.15 Stormwater interception ratio R_r varying with storage capacities and water demands. ·· 35
Fig. 3.16 Stormwater interception ratio R_r varying with water demands and roof areas. ·· 36
Fig. 3.17 Stormwater interception ratio R_r varying with roof areas and storage capacities. ·· 36
Fig. 4.1 Comparisons of water supply reliability and stormwater interception ratio of stochastic model and the estimated formula with varying storage capacities. ·· 39
Fig. 4.2 Comparisons of water supply reliability and stormwater interception ratio of stochastic model and the estimated formula with varying water demands. ·· 40
Fig. 4.3 Comparisons of water supply reliability and stormwater interception ratio of stochastic model and the estimated formula with varying contributing ratios. ·· 40
Fig. 4.4 Annual average precipitation of present and future climate data at 6 sites. ·· 43
Fig. 4.5 Annual average stormwater depth of present and future climate data at 6 sites. ·· 44
Fig. 4.6 Water supply reliability of future climate date at 6 sites. ············ 45

List of Tables

Table 2.1 Information of future climate models data ······································· 7

Table 4.1 R^2 and RMSE between stochastic model and the estimated formula ·· 38

빗물이용시설의 추계학적 해석 및 기후변화 적응시설로서의 활용성 분석

심 인 경

부 경 대 학 교 대 학 원 지 구 환 경 시 스 템 과 학 부
환 경 공 학 전 공

요 약

빗물이용시설 (Rainwater Harvesting System, RHS)은 도시 물 공급 및 수자원 관리를 위한 효과적인 저 영향 개발 기법 중 하나이다. 본 연구에서는 강우의 확률적 특성에 초점을 맞추어, RHS의 물 공급을 위한 신뢰도 및 수자원 관리를 위한 강우유출수 처리 효율을 정량화하기 위한 확률모델을 제시하고자 하였다. Master Key Fokker-Planck 방정식 (Master Key Fokker-Planck Equation, MKFPE)을 사용하여 추계론적 상미분 방정식으로 구성된 지배방정식은 시설에 존재하는 물의 비율에 따른 확률밀도함수 (Probabilistic Density Function, PDF)를 상태변수로 하는 결정론적 편미분 방정식으로 변환된다. 이를 통해 RHS의 다양한 성능을 분석하며, 매개변수에 따른 물 공급 신뢰도와 강우유출수 처리비 산정을 위한 공식을 제안하였다. 마지막으로 제안된 모형과 다양한 기후변화 시나리오를 이용하여 미래의 물 공급 신뢰도와 RHS가 기후변화의 악영향을 상쇄시켜 미래 강우유출수가 어느 정도 처리되는지를 시설의 제원과 강우의 특성을 고려하여 분석하였다. 본 연구의 결과는 향후 RHS의 성능평가, 최적 설계 및 기후변화 영향 분석에 유용한 도구가 될 것으로 기대된다.

Ⅰ. Introduction

1.1 Background

Pollutants in urban areas are largely classified into point pollution sources and non-point pollution sources, where non-point pollution source refers to a pollutant that is difficult to know the exact source because it is washed and discharged from a large area, such as rainwater. Non-point pollution sources include agricultural lands, grazing, urban streets, forests, suburbs and so on. Pollutants near the soil surface or surface are washed by rainwater and flow into the water system as runoff.

Rapid industrial development and urbanization in Korea have been taking place since the 1960s, and urbanization has been intensified, leading to an increase in impervious area and population density. In this way, the urbanization of the urban area has changed the water cycle system compared to the past (Shuster et al., 2005; Kim et al., 2012). Urbanized lands with high impermeability will have large influx of non-point pollutants during rainfall events, affecting surface water and groundwater (Menció and Mas-Pla, 2008). As a result, flood damage is increasing, water resources are difficult to secure, river water quality deteriorates, and groundwater depletion is increasing (Park and Cho, 2015).

In order to solve the problems caused by the water cycle distortion due to urbanization and to manage the water resources sustainably, the urban water cycle management paradigm of Low Impact Development (LID) technique is introduced in USA, Europe, Canada, and Australia, and it is proceeding (Ahiablame et al., 2013; Zhang et al., 2013; Chui et al., 2016; Mao et al., 2017; Eckart et al., 2018). LID technique is a method to preserve the characteristics of the existing area by infiltrating, filtering, and storing the rainwater to the ground without the direct discharge of the rainwater so as to be similar to the water cycle system in the natural state. It is an eco-friendly rainwater management technique that can sustain natural ecosystems and biological resources including rivers. As such, LID is currently being applied with great interest in Korea. It is actively implemented to urban water cycle management, non-point sources pollutant management, and stormwater management.

1.2 Objectives

Among various LID application technologies, the Rainwater Harvesting System (RHS) is becoming an increasingly important alternative to water supply in water-scarce areas (Thomas, 1998; Kahinda et al., 2007; Che-Ani et al., 2009), and in addition to the water supply business, there is an advantage that it can be effectively applied to water resources management by reducing or reusing stormwater that flows directly into urban impervious surfaces (Jennings et al., 2012; Keem et al., 2014). RHS should be actively installed to preserve natural water cycle without compromising the functionality of a city. RHS is considered to be a sustainable and efficient means of managing urban water resources (Butler et al., 2010; Choi et al., 2011; Ward et al., 2012).

Among the cases of RHS that are currently installed worldwide, in Japan, RHS has been used to achieve effects such as flood protection, water conservation, river pollution prevention, and construction pipe system cost reduction in addition to water supply in the city since 1985 (Zaizen et al., 2000). In Australia, RHS has been installed for many years in arid inland areas. Recently, due to drought and climate change, RHS has become an important alternative source of fresh water, and the installation of RHS is increasing (Eroksuz and Rahman, 2010). In the United States, attempts have been made to actively use rainwater in California for the first time, and the use of rainwater is increasing in island areas such as Guam (Han, 2002). Meanwhile, in Germany, a rainwater management infrastructure has been established to prevent flooding in cities, and a rainwater storage facility for groundwater reclamation is also installed and managed. Unlike other countries, most German cities use groundwater as their source of water, making it one of the most active countries for rainwater use (Lee, 2004).

As the interest in reuse of water is rapidly increasing, there is an increasing tendency to promote the reuse of water and to utilize water resources efficiently, and therefore, many related studies have been conducted (Palla et al., 2011; Palla et al., 2012; Campisano et al., 2017). Ghisi (2006) assessed the actual water availability, estimated the potential for potable water savings, and discussed water availability indicators that demonstrate the benefits of using rainwater. In addition, stochastic rainfall models for rainwater use assessment in South Africa with low water access rates have been developed (Cowden et al., 2008). Basinger et al. (2010) introduced the Storage and Reliability Estimation Tool (SARET), which evaluates the reliability of RHS. Guo and Guo (2018) proposed a probability model to quantify the water supply reliability and stormwater capture ratio of RHS, and tried to adjust the size of RHS using the probability model and to evaluate its performance (Sample and Liu, 2014). The RHS is evaluated using various models, and studies such as RHS design, capacity, installation efficiency and RHS optimal design capacity are being actively conducted (Guo and Batez, 2007; Su et al., 2009; Okoye et al., 2015).

In Korea, there is a statute for the installation of RHS and related researches are being carried out. Choi et al. (2011) established detailed procedures for the design of rainwater use facilities using SARET to assess the reliability of RHS and to quantify the reduction efficiency of stormwater and annual tap water use. In addition, Keem et al. (2014) presented a method for estimating model parameters based on the data available in Korea to increase the domestic applicability of the reliability assessment model proposed by Choi et al. (2011), and analyzed the annual average and seasonal reliability of RHS. Hydrological evaluation of RHS has also been carried out through long-term continuous runoff analysis (Yoo et al., 2008; Kim et al., 2008). Based on the economic assessment of the introduction of RHS, studies such as estimating the optimal design capacity have also been conducted (Hong et al., 2005; Park et al., 2007; Kim et al., 2014; Kang et al., 2015; Baek et al., 2018). However, researches that analyze the behavior of RHS probabilistically are rare, and comprehensive and systematic studies are still insufficient compared to studies of developed countries in the RHS field.

Therefore, this study focuses on the probabilistic characteristics of rainfall and suggests a probability model considering the inflow and loss of RHS. Using the derived probability model, the reliability for water supply and the stormwater capture efficiency for water resource management are quantified. The formula for estimating the water supply reliability and the stormwater interception ratio with respect to RHS parameters is also proposed. Using the proposed model, the future water supply reliability of RHS and the capability of stormwater capture under various climate change scenarios are analyzed to investigate the applicability of RHS to offset the adverse effect of climate change.

Ⅱ. Materials and methods

2.1 Data

Rainfall observation data were obtained from the Korea Meteorological Administration Automated Synoptic Observing System (ASOS) data. The daily ASOS meteorological data are available from KMA website (http://data.kma.go.kr). Rainfall data from six major Korean sites (Busan, Daegu, Daejeon, Gwangju, Incheon, Seoul) were used. The data period is 40 years from 1979 to 2018.

In this study, dynamically down-scaled present and future climate data (KOR-11) were used with a horizontal resolution of 12.5-km in the East Asia region including the Korean Peninsula. Future climate change scenarios in KOR-11 were applied to Representative Concentration Pathways (RCP) 4.5 and 8.5, and two GCMs including MPI-ESM-LR (Max Plank Institute Earth System Model-Low Resolution) and HadGEM2-AO (Hadly Center Global Environmental Model version 2 coupled with the Atmosphere-Ocean) and four RCMs (MM5, RegCM4, RSM, WRF) were used. Therefore, a total of 16 future ensembles were used. In this study, dynamically down-scaled present and future climate data (KOR-11) were used with a horizontal resolution of 12.5-km in the East Asia region including the Korean Peninsula. Future climate change scenarios in KOR-11 were applied to Representative Concentration Pathways

(RCP) 4.5 and 8.5, and two GCMs including MPI-ESM-LR (Max Plank Institute Earth System Model-Low Resolution) and HadGEM2-AO (Hadly Center Global Environmental Model version 2 coupled with the Atmosphere-Ocean) and four RCMs (MM5, RegCM4, RSM, WRF) were used. Therefore, a total of 16 future ensembles were used (see Table 2.1).

Table 2.1 Information of future climate models data

GCMs	RCMs	Scenarios	Spatial Resolution	Temporal Resolution	Temporal Scale
MPI-ESM-LR (ML)	MM5	RCP 4.5 RCP 8.5	12.5-km	3-hour (365-Day in 1-year)	Present: 1981~2010 Future: 2021~2050
	WRF				
	RegCM4				
	RSM				
HadGEM2-AO (H2)	MM5				
	WRF				
	RegCM4			3-hour (360-Day in 1-year)	
	RSM				

2.2 EPA SWMM

The EPA-Storm Water Management Model (SWMM), the most widely used in the field, is widely used for hydrological simulation.

Since more than 8 LID facilities can be simulated within the model, it is possible to compare and analyze stormwater in the watershed according to the characteristics of each facility. However, in order to use SWMM, a model must be constructed by inputting parameters of LID facilities and other parameters. This can be rather difficult and complicated for non-experts. Recently, several researchers have derived a probabilistic model of several LID facilities, focusing on the stochastic characteristics of rainfall to estimate stormwater interception ratio more easily even without SWMM implementation (Guo and Baetz, 2007; Kim et al., 2012; Zhang and Guo, 2012a; Zhang and Guo, 2012b; Guo et al., 2014; Sample and Liu, 2014; Zhang and Guo, 2014a; Zhang and Guo, 2014b; Becciu et al., 2016; Guo and Gao, 2016; Guo et al., 2017; Guo and Guo, 2018). Therefore, in this study, a probabilistic model of rainwater utilization facilities was derived and compared with SWMM simulation results, which are most widely used for hydrological simulation, to verify the results.

2.3 Stochastic model for dynamic water balance in RHS

he characteristics of rainfall play an important role in RHS, and reflecting the water remaining in the existing RHS storage and the newly inflow water will be key to model dynamic water balance in

RHS. In this study, a stochastic model for dynamic water balance in RHS was derived based on a simple storage equation as follows:

$$\frac{ds}{dt} = \eta(s,t) = \frac{1}{W_c}[I(R,s) - L(s)] \quad (1)$$

Where W_c is the capacity of the RHS TANK storage (mm), I (mm/day) is the amount of rainwater supplied to the RHS storage from the rainfall R, and s is the ratio of the water remaining in the RHS storage, that is, the normalized water depth. The loss rate L (mm/day) is the function related to the amount of demand used for water supply. Fig. 2.1 shows a schematic of the RHS.

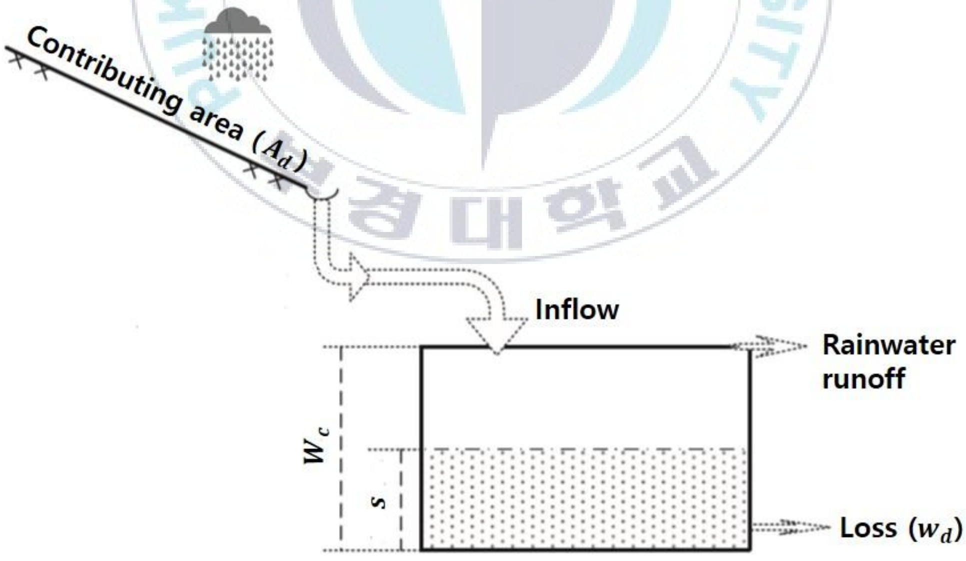

Fig. 2.1 Schematic of inflow into and outflow from a RHS.

The exponential probability density function (PDF) for daily rainfall R (mm/day) is shown in Equation (2) and Fig. 2.2, respectively.

$$f_R(R) = \frac{\lambda}{R_m} e^{-R/R_m} \quad \cdots\cdots (2)$$

Where, λ is the probability that rainfall will occur on a day (that is, the probability of rainfall occurrence in a day), and the probability that rainfall will not occur on a day (P_{R_o}) is $1-\lambda$이다. In Fig. 2.2, R_m (mm/day) means the mean value of the rainfall depth on the rainy day, and S_d is the incipient loss (Kim et al., 2011).

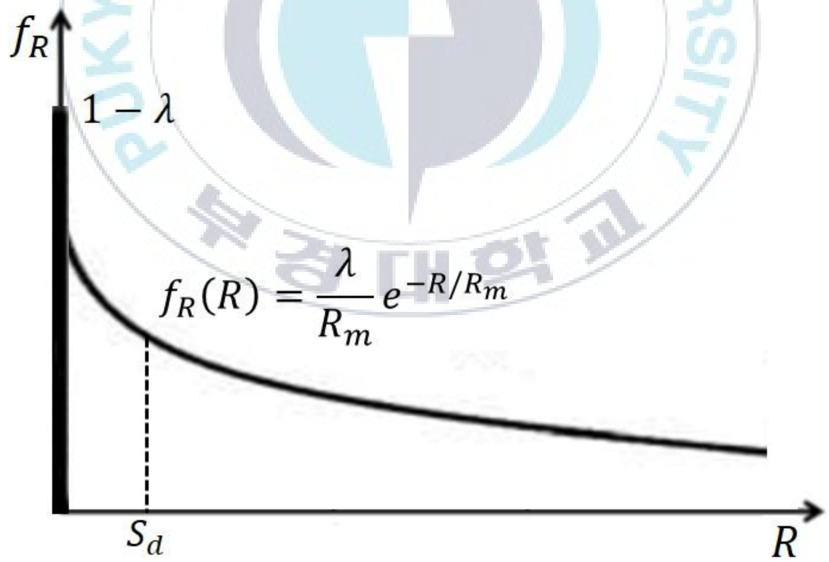

Fig. 2.2 Probability density function of rainfall depth.

The contribution drainage area (mainly roof) is assumed to be impermeable, and the outflow Q (mm/day) refers to the stormwater depth occurring in the contributing area of RHS. If the outflow Q is smaller than the surface depression depth S_d (mm/day), the outflow does not occur, and the outflow occurs only when outflow is larger than S_d, which is expressed by Equation (3). Note that not all of the generated Q enters RHS storage but only the amount that can be received by the capacity of RHS enters and the remaining is overflowed (Kim and Han, 2010).

$$\begin{aligned} Q &= 0 \qquad , \quad \text{for } R < S_d \\ &= \phi^{-1}(R - S_d) , \quad \text{for } R \geq S_d \end{aligned} \quad \cdots\cdots (3)$$

Where ϕ means the ratio (A_R/A_d) of the bottom area of the RHS storage (A_R) to the catchment area (A_d), and the PDF of the outflow Q can be expressed by Equation (4) through the PDF of the rainfall R.

$$f_Q(Q) = \frac{\lambda}{R_m} e^{-(Q+S_d)/R_m} \quad \cdots\cdots (4)$$

In this case, when the probability that the outflow will occur on a day is defined by λ', the probability that the outflow does not occur, that is, the probability $(1-\lambda')$ that $Q=0$ is equal to the sum of the probability of rainlessness and the probability that the rainfall does not exceed the incipient loss S_d, and can be expressed as follows:

$$P_Q(0) = \mathrm{Prob}[Q=0] \quad \cdots\cdots (5)$$
$$= \mathrm{Prob}[R=0] + \mathrm{Prob}[R \leq \ S_d]$$
$$= 1 - \lambda'$$

Where the probability of outflow λ' is $\lambda e^{-S_d/R_m}$.

If an outflow occurs, an inflow into RHS occurs, in which the inflow is allowed only as much as the remaining space of RHS. Therefore, it is important to consider the amount of water currently remaining in RHS. If the free space remaining in the RHS can accommodate Q, the inflow I entering RHS will be equal to Q, but if the remaining space cannot accommodate all Q, only the remaining space is allowed. This can be expressed as follows:

$$I = 0 \quad , \quad \text{for } R < S_d \quad \cdots\cdots (6)$$
$$= \phi^{-1}(R - S_d) \ , \quad \text{for } \phi^{-1}(R - S_d) < F(s)$$
$$= F(s) \quad , \quad \text{for } \phi^{-1}(R - S_d) > F(s)$$

Where the remaining space of RHS is denoted by $F(s)$ and can be expressed as follows:

$$F(s) = (1 - s)\, W_c / \triangle t \quad \cdots\cdots (7)$$

Note that the probability $P[I=0]$ that there is no inflow to RHS on a day, such as the probability that the outflow in Equation (5) will not occur, is as follows:

$$P[I=0]=P[R=0]+P[R \leq \ S_d] \qquad (8)$$
$$=1-\lambda'$$

The probability P_F that $F(s)$ will inflow to RHS on a day, that is, the probability of $I=F(s)$, can be expressed as follows:

$$P[I=F(s)]=P_{F(s)} \qquad (9)$$
$$=P[S_d+\phi F(s)<R]$$
$$=\lambda' G(s)$$

In other words, P_F can simply be expressed as $\lambda' G(s)$. Where $G(s)$ can be expressed as Equation (10), and $G(s)$ is dimensionless.

$$G(s)=e^{-\phi F(s)/R_m} \qquad (10)$$

The probability distribution function for the remaining inflows $(\phi^{-1}(R-S_d))$ except for both extreme cases $(I=0$ and $I=F(s))$ can be derived as follows using the same relation as $f_I \ \ dI=f_R \ \ dR$:

$$f_I=f_R(R)\cdot \ \frac{dR}{dI} \qquad (11)$$
$$=\frac{\lambda'}{r_m}e^{-I/r_m}$$

Where r_m (mm/day) is introduced to simplify the equation as follows:

$$r_m = \frac{R_m}{\phi} \quad \text{(12)}$$

As a result, the PDF for inflow to RHS can be presented as shown in Fig. 2.3.

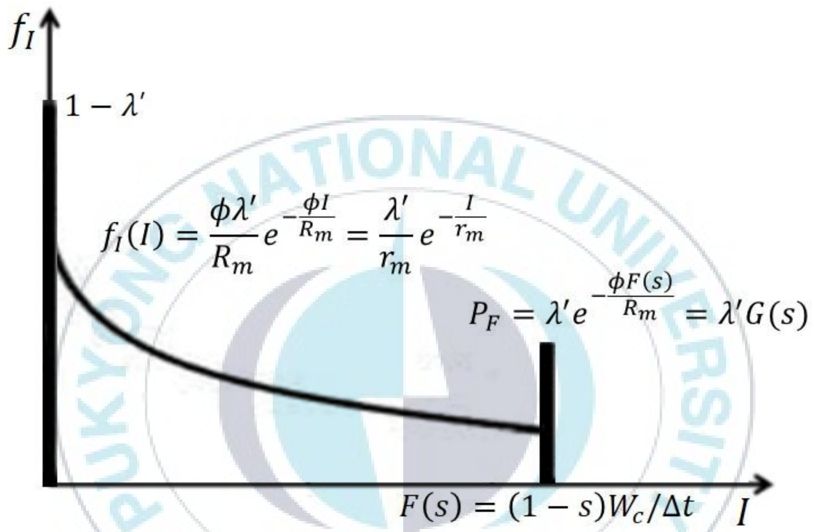

Fig. 2.3 Probability density function of inflow.

Rainwater stored in RHS can be used for water supply, and the amount of water used is the loss function $L(s)$ of RHS. The loss function $L(s)$ is defined in two cases (see Fig. 2.4):

$$\begin{aligned} L(s) &= \frac{w_d}{s^*} s = \frac{W_c}{\Delta t} s\,, \quad \text{for } 0 < s < s^* \quad \text{(13)} \\ &= w_d \quad\quad\quad\quad\ , \quad \text{for } s^* < s \le 1 \end{aligned}$$

Where w_d is the predefined water supply demand (mm/day). If enough rainwater is stored in RHS, a predefined w_d is supplied, but otherwise only the stored water is supplied. Hence, the threshold value $s*$ of rainwater stored in RHS can be expressed as follows:

$$s* = \frac{w_d \triangle t}{W_c} \quad \cdots\cdots (14)$$

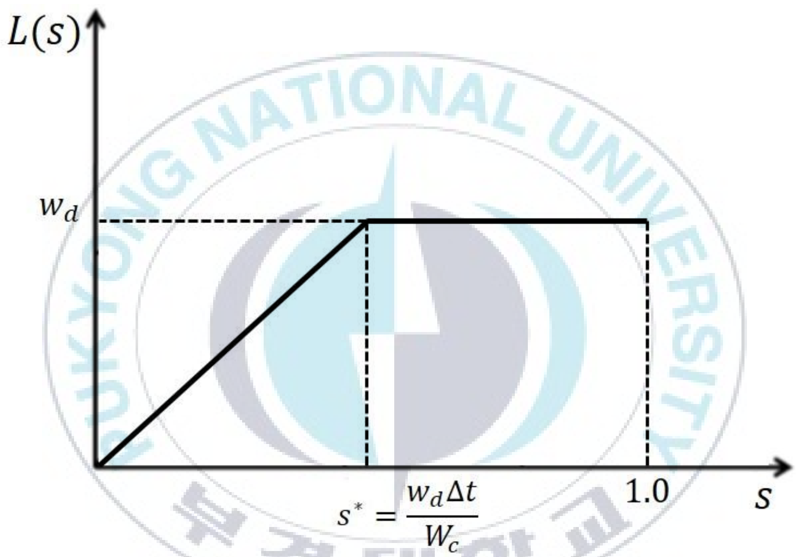

Fig. 2.4 Loss function.

Based on Kavvas (2003), the governing Equation (1) of RHS can be transformed into the Master key Fokker-Planck equation as follows:

$$\frac{\partial p}{\partial t} = -\frac{\partial}{\partial s}\left[\left(<\eta> - \int_o^t cov[\eta_t; \frac{\partial \eta}{\partial s}|_{t-\tau}]d\tau\right)p\right] + \frac{\partial}{\partial s}\left[\left(\int_o^t cov[\eta_t;\eta_{t-\tau}]d\tau\right)\frac{\partial p}{\partial s}\right] \quad \cdots\cdots (15)$$

where $p(s,t)$ is the state variable of Equation (15) and is the PDF of the normalized water depth of RHS. The Equation (15) can be fully expressed as follows:

$$\frac{\partial p}{\partial t} = -\frac{\partial}{\partial s}[(\frac{\lambda' R_m}{\phi W_c}(1-G) - \frac{s}{\triangle t} - \frac{\theta_1 \lambda' G}{2 W_c \triangle t}(\frac{\lambda' R_m}{\phi}(1-G) - F))p(s,t)] \quad \cdots (16)$$

$$+\frac{\partial}{\partial s}[(\frac{\theta \lambda' R_m^2}{\phi^2 W_c^2}(1-G-\frac{\phi FG}{R_m}) - \frac{\theta(\lambda')^2 R_m^2}{2\phi^2 W_c^2}(1-G)^2) \times \frac{\partial p(s,t)}{\partial s}], \quad \text{for } s < s^*$$

$$= -\frac{\partial}{\partial s}[(\frac{\lambda' R_m}{\phi W_c}(1-G) - \frac{w_d}{W_c} - \frac{\theta_1 \lambda' G}{2 W_c \triangle t}(\frac{\lambda' R_m}{\phi}(1-G) - F))p(s,t)]$$

$$+\frac{\partial}{\partial s}[(\frac{\theta \lambda' R_m^2}{\phi^2 W_c^2}(1-G-\frac{\phi FG}{R_m}) -$$

Equation (16) can be more simply expressed as follows:

$$\frac{\partial p}{\partial t} = -\frac{\partial}{\partial s}[(\frac{\lambda' r_m}{W_c}(1-G) - \frac{s}{\triangle t} - \frac{\theta_1 \lambda' G}{2 W_c \triangle t}(\lambda' r_m(1-G) - F))p(s,t)] \quad \cdots\cdots\cdots (17)$$

$$+\frac{\partial}{\partial s}[(\frac{\theta \lambda' r_m^2}{W_c^2}(1-G-\frac{FG}{r_m}) - \frac{\theta(\lambda')^2 r_m^2}{2 W_c^2}(1-G)^2) \times \frac{\partial p(s,t)}{\partial s}], \quad \text{for } s < s^*$$

$$= -\frac{\partial}{\partial s}[(\frac{\lambda' r_m}{W_c}(1-G) - \frac{w_d}{W_c} - \frac{\theta_1 \lambda' G}{2 W_c \triangle t}(\lambda' r_m(1-G) - F))p(s,t)]$$

$$+\frac{\partial}{\partial s}[(\frac{\theta \lambda' r_m^2}{W_c^2}(1-G-\frac{FG}{r_m}) - \frac{\theta(\lambda')^2 r_m^2}{2 W_c^2}(1-G)$$

Where θ_1 is the scale of fluctuation of daily I_t and $\partial I/\partial s$ time series, and θ is the scale of fluctuation of daily η_t time series, respectively.

$$\theta_1 = 2\int_0^\infty \rho_1(\tau) d\tau = |\rho_1(0)| \Delta t \quad \cdots\cdots (18)$$

$$\theta = 2\int_0^\infty \rho(\tau)d\tau \quad (19)$$

Where $\rho_1(\tau)$ is the cross-correlation function of daily I_t and $\partial I/\partial s$ time series at lag-τ, and $\rho(\tau)$ is the auto-correlation function of daily η_t time series at lag-τ, respectively.

In order to analyze numerically the stochastic model derived above, Equation (15) and (17) can be expressed more simply as follows:

$$\frac{\partial p}{\partial t} = -\frac{\partial}{\partial s}[Ap] + \frac{\partial}{\partial s}[D\frac{\partial p}{\partial s}] \quad (20)$$

Where $A(s)$ and $D(s)$ are called respectively the advection and dispersion coefficients, as the form of Equation (20) closely resembles the advection-dispersion equation. The Equation (20) is basically a continuity equation and the state variable of the Equation (20) is the probability density.

2.4 Steady-state PDF for normalized depth of RHS

According to Chang and Cooper (1970), one can finally obtain the steady-state PDF of the normalized water depth in RHS under stochastic rainfall forcing and RHS and catchment parameters as follows:

$$p(s) = N_o \exp\left[\int_0^s \frac{A(\xi)}{D(\xi)} d\xi\right] \quad \text{(21)}$$

Where N_o can be expressed as a constant of integration or a normalization constant as follows:

$$N_o = \int_0^1 p(s) ds = 1 \quad \text{(22)}$$

Note that the steady-state PDF of the normalized water depth in RHS is expressed as a function of rainfall characteristics such as rainfall frequency, average rainfall in a rainy day, and scale of fluctuation of daily rainfall time series, and RHS properties such as storage capacity, water demand, RHS area, contributing area, and incipient loss.

The state variable $p(s,t)$ of Equation (20) is strictly a probability density. However, the normalized water depth in RHS has a probability mass at $s=0$ or $s=1$. Therefore, it is necessary to consider the probability mass separately. Regardless of the amount of water remaining in TANK the previous day, the probability that s will be zero is always p_0. Since the occurrence probability of the outflow Q is λ', the outflow Q occurs on average once every $1/\lambda'$-day. Assuming that the occurrence of the runoff event follows the poisson distribution, the PDF of the time T (day) between runoff events can be described as follows:

$$f(T) = \lambda' e^{-\lambda'/T} \quad \text{(23)}$$

If the time between runoff events is greater than $T_a = W_c / w_d$, then the amount of rainwater remaining in RHS is unconditionally zero. Hence, the probability mass p_0 can be written as follows:

$$\begin{aligned} p_0 &= P[T > T_a] \\ &= e^{-\lambda' T_a} \end{aligned} \quad \text{(24)}$$

Similarly, regardless of the amount of water remaining in TANK the previous day, the probability that s will always be 1 is p_1. The probability mass p_1 can be estimated to be the probability of rainfall exceeding the critical rainfall depth that satisfies $W_c + w_d \Delta t = \phi^{-1}(R_c - S_d)\Delta t$. The critical rainfall depth is as follows:

$$R_c = S_d + \frac{\phi}{\Delta t}(W_c + w_d \Delta t) \quad \text{(25)}$$

Hence, the probability mass p_1 can be written as follows:

$$\begin{aligned} p_1 &= P[R > R_c] \\ &= \lambda e^{-R_c / R_m} \end{aligned} \quad \text{(26)}$$

After determining above all parameters, the steady-state PDF of the normalized water depth in RHS can be obtained numerically.

2.5 Water supply reliability and stormwater interception ratio

What we most want to know from the RHS installation is how much water we can supply and how much stormwater can be captured. Using the steady-state PDF of the normalized water depth in RHS, the reliability of how much water can be supplied and how much stormwater can be captured can be derived. The water supply reliability R_e can be expressed as follows:

$$R_e = \frac{E[L]}{E[D]} = \frac{\int_0^1 L(s)p(s)ds}{w_d} \qquad (27)$$

Where $E[D]$ is the total amount of water desired to be supplied from RHS, and $E[L]$ is the total amount of actual water supplied from RHS.

Meanwhile, the stormwater interception ratio R_r is can be written as follows:

$$R_r = \frac{E[L]}{E[Q]} = \frac{\int_0^1 L(s)p(s)ds}{\lambda \frac{R_m}{\phi} e^{-S_d/R_m}} \qquad (28)$$

Where $E[Q]$ means the amount of outflow from the contributing area, and stormwater interception ratio can be expressed as a function of supply and outflow.

As a result, the water supply reliability and stormwater interception ratio can be estimated using only the rainfall characteristic parameter and the RHS characteristic parameter using the derived probabilistic model. Accordingly, if rainfall data by site is inputted, the rainfall characteristic parameters are applied accordingly to estimate water supply reliability and stormwater capture efficiency according to various climates.

Ⅲ. Results

3.1 Stochastic model verification

In this section, the results of numerical models and probability models are compared with each other to examine the adequacy of probability models. Water supply reliability and stormwater interception ratio were calculated every five years using rainfall data (1979-2018; 40 years) from March to November (see Fig. 3.1 and 3.2). The water supply reliability shows a relatively similar result, although the two models are not perfectly consistent with each other. Stormwater interception ratios are in good agreement with the results of the two models.

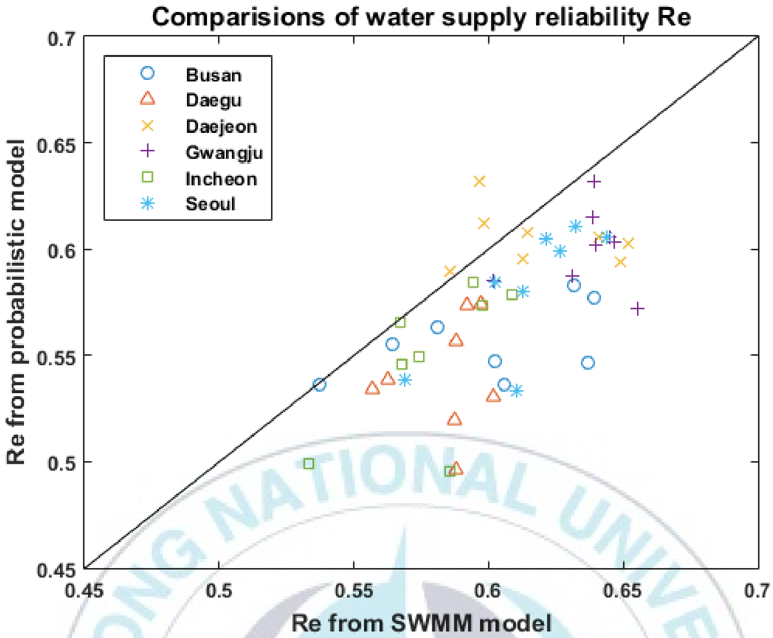

Fig. 3.1 Comparisons of water supply reliability R_e in 6 sites.

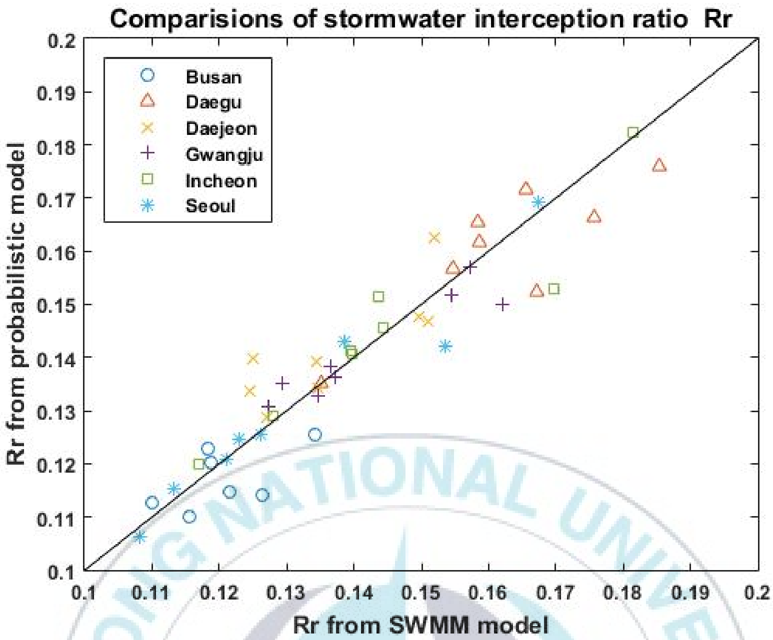

Fig. 3.2 Comparisons of stormwater interception ratio R_r in 6 sites.

When comparing the reliability values of the SWMM and the probability model, the water supply reliability did not fit perfectly, but on average, the results were relatively similar. On the other hand, the stormwater interception ratio was confirmed to be in good agreement with the SWMM results.

When analyzing several sites, it was confirmed that the derived probabilistic model appeared similar to the SWMM results. To examine the adequacy of the probabilistic model in detail, using the data from the Busan site to explore the agreement between the two model results for the change in the RHS parameters . Fig. 3.3-3.5 shows the comparison of water supply reliability and stormwater interception ratio for various values of RHS storage capacity, demand, and catchment area. Parameters other than the parameters that changed for the probability model verification were fixed at the default values.

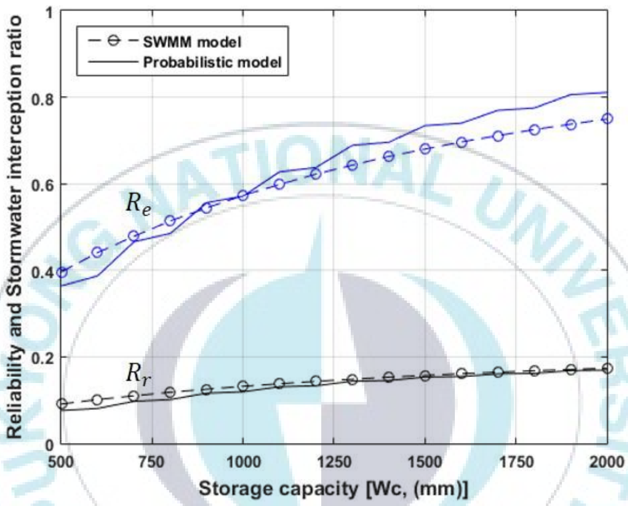

Fig. 3.3 Water supply reliability and stormwater interception ratio of RHS with varying storage capacities.

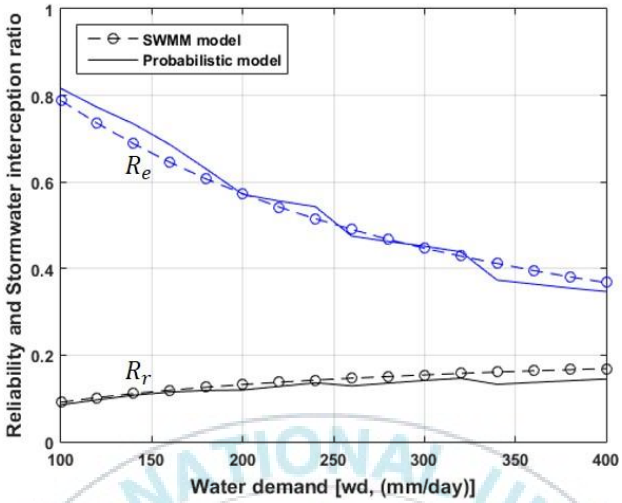

Fig. 3.4 Water supply reliability and stormwater interception ratio of RHS with varying water demands.

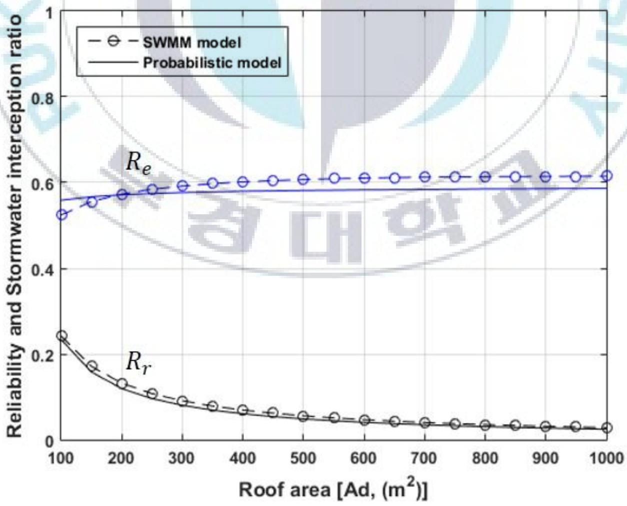

Fig. 3.5 Water supply reliability and stormwater interception ratio of RHS with varying roof areas.

In Figs. 3.3–3.5, the dotted line represents the numerical model and the solid line represents the probability model. The blue line shows the result of water supply reliability and the black line shows the result of stormwater interception ratio. As the capacity of storage capacity increases, more rainfall can flow into RHS. As a result, the reliability of the supply of demand is gradually increased. As storage capacity increases, stormwater interception ratios also increase with water supply reliability because more rainwater is converted to supply (see Fig. 3.3). Increasing water demand with fixed storage capacity reduces water supply reliability, but improves stormwater interception ratios due to the conversion of rainwater supply (see Fig. 3.4). Increasing catchment area leads to an increase in RHS inflow, which improves water supply reliability, whereas increasing RHS inflow adversely affects stormwater interception ratios (see Fig. 3.5). The results of Figs. 3.3–3.5 show that the proposed probabilistic model reproduces the numerical model results very well for various situations. As a result, by simply applying the probabilistic model proposed in this study, it is easy to estimate the RHS water supply reliability and stormwater interception ratio without using complicated and inconvenient SWMM.

3.2 Further analysis of stochastic RHS model

3.2.1 Sensitivity analysis by parameter

In Section 3.1, the derived probabilistic models are compared with the SWMM simulation results. In this section, the behavior of the facility according to the parameters is analyzed when changing by parameter. First, cumulative distribution function (CDF), mean and p_0 of s for various parameter ranges were compared and analyzed. Figs. 3.6–3.8 compare the CDFs of s for various cases by parameter, and Figs. 3.9–11 show the mean of s and p_0 in various ranges for each parameter.

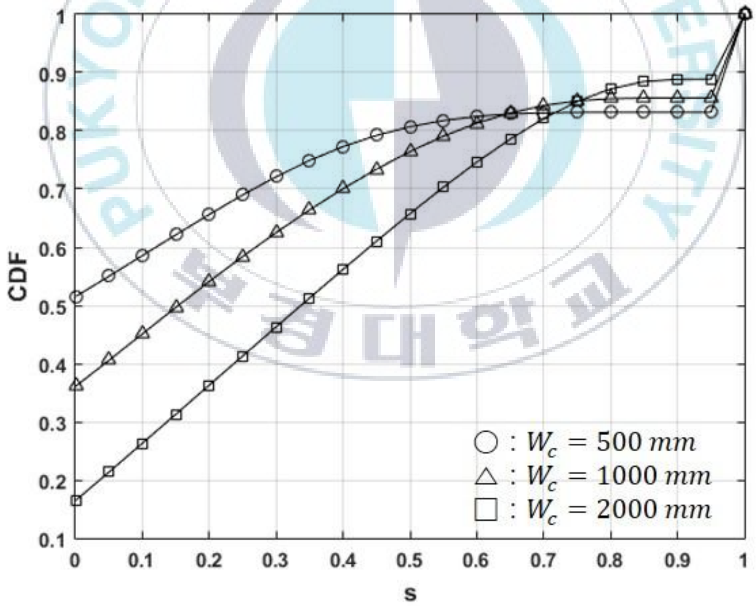

Fig. 3.6 CDF of s with varying storage capacities.

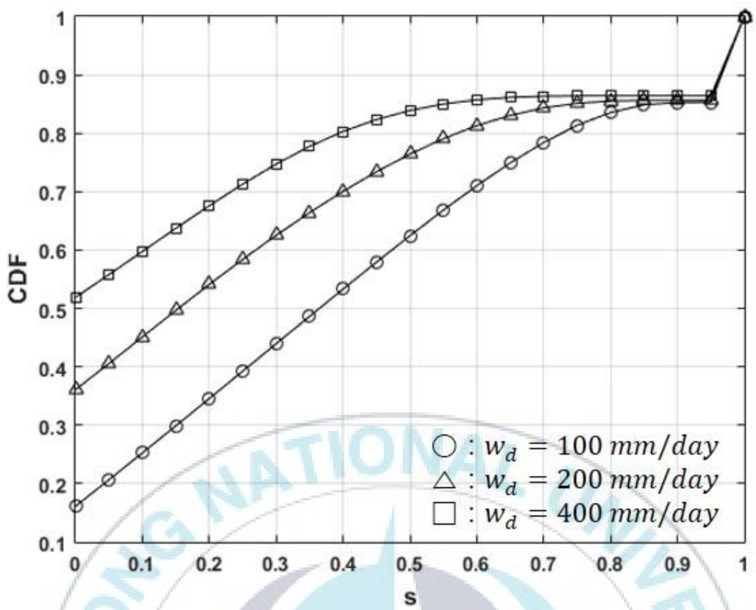

Fig. 3.7 CDF of s with varying water demands.

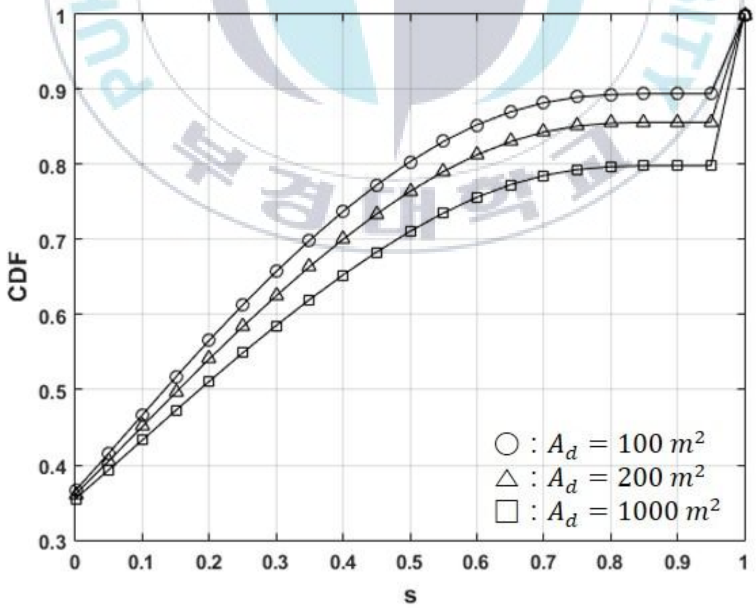

Fig. 3.8 CDF of s with varying roof areas.

Figs. 3.6–3.8 show the CDFs of normalized water depth in RHS for various parameters. As the capacity of the RHS decreases, the rainwater in the storage depletes faster, leading to the formation of CDFs as shown in Fig. 3.6. If the required water demand increases, the probability of depletion of the remaining water in the RHS will increase, resulting in CDFs shaped like Fig. 3.7. In light of the similarity of CDF change patterns in Fig. 3.6 and 3.7, the capacity of RHS and the demand for water from RHS have a similar effect on the condition of normalized water depth in RHS. However, the change in CDF shape of the normalized water depth in RHS with respect to the change of the catchment area is different from the two cases. It can be seen that the change of catchment area affects the probability that the stored rainwater is sufficient more than the probability of running out of stored rainwater (see Fig. 3.8).

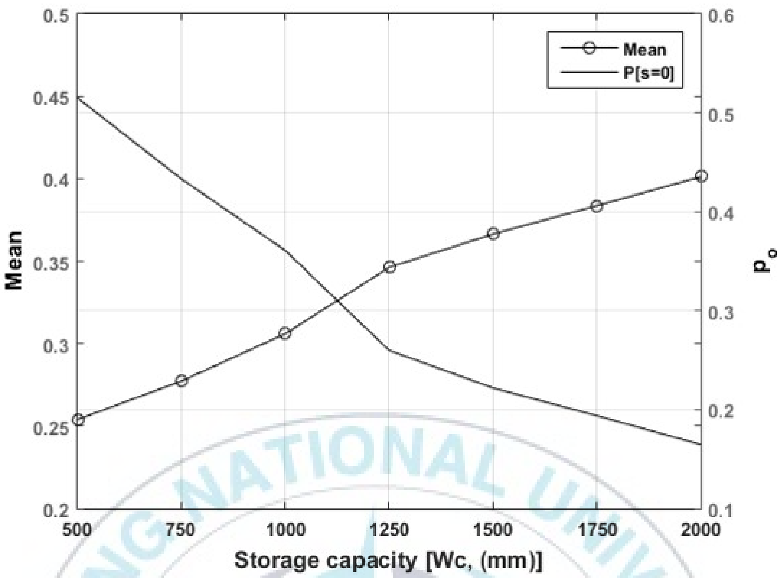

Fig. 3.9 Mean of s and p_0 with varying storage capacities.

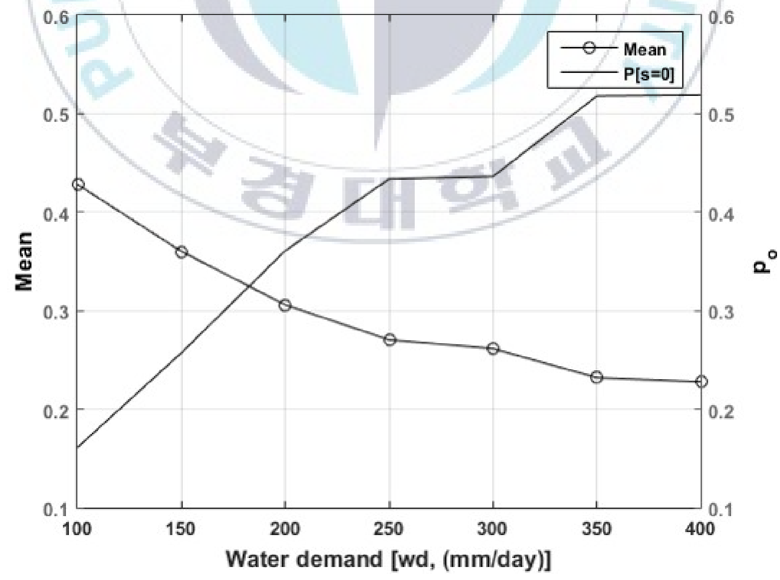

Fig. 3.10 Mean of s and p_0 with varying water demands.

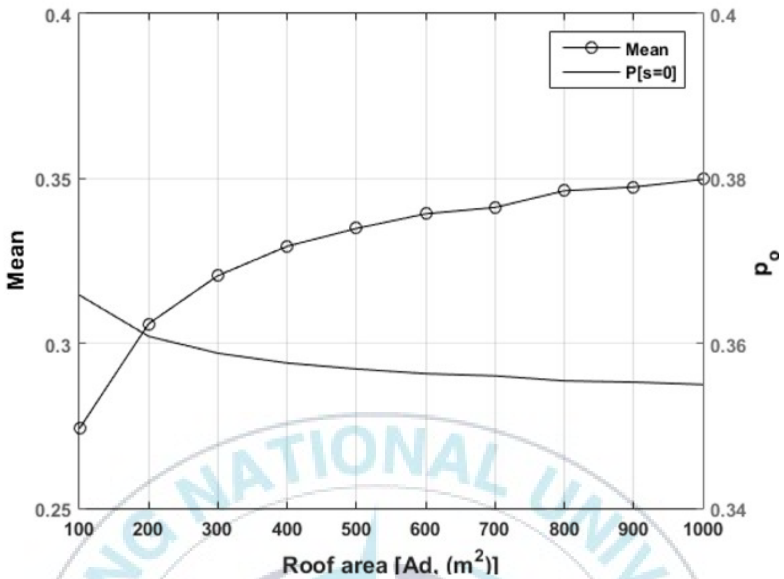

Fig. 3.11 Mean of s and p_0 with varying roof areas.

Figs. 3.9–3.11 show the average of the normalized water depth in RHS and the probability when the normalized water depth is 0 over the range of various parameters. As the RHS capacity increases, more rainwater can be stored, so the average of normalized water depth in RHS gradually increases, whereas the probability of zeroing normalized water depth in RHS gradually decreases (see Fig. 3.9). As the water demand increases, the stored rainwater is depleted at a faster rate, so the average of the normalized water depth in RHS decreases, and the probability of normalized water depth in RHS being zero moves in the increasing direction (see Fig. 3.10). As the catchment area increases, the inflow of RHS increases, so the average of normalized water depth in RHS increases gradually, and the probability when normalized water depth in RHS is zero decreases (see Fig. 3.11). However, it is worth noting that the catchment area has a relatively small effect on the behavior of normalized water depth in RHS compared to the capacity and water demand of RHS. Therefore, it can be seen that the normalized water depth in RHS is mainly determined by the RHS capacity and water demand rather than the catchment area.

3.2.2 Sensitivity analysis by parameter combination

Figs. 3.12–3.14 and 3.15–3.17 show the water supply reliability and stormwater interception ratio for various ranges of parameters calculated using the proposed probabilistic model.

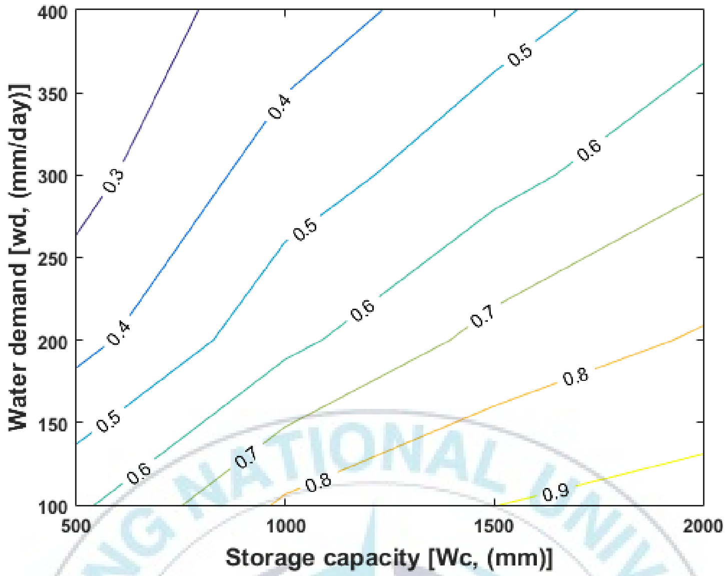

Fig. 3.12 Water supply reliability R_e varying with storage capacities and water demands.

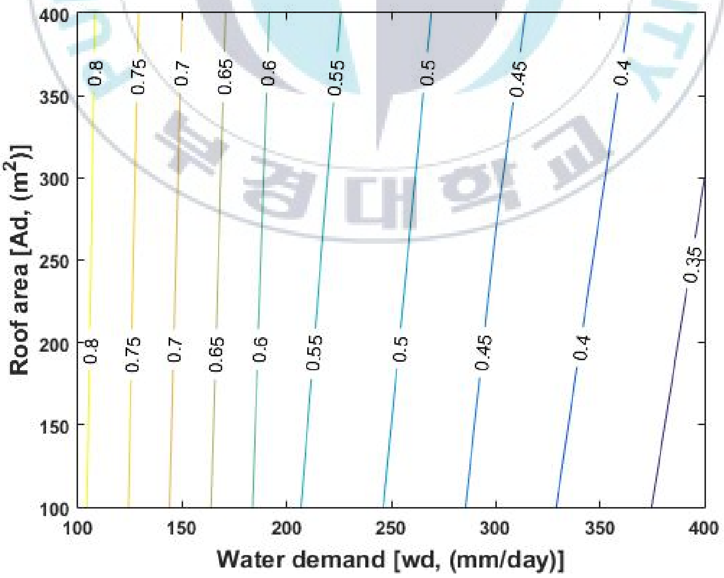

Fig. 3.13 Water supply reliability R_e varying with water demands and roof areas.

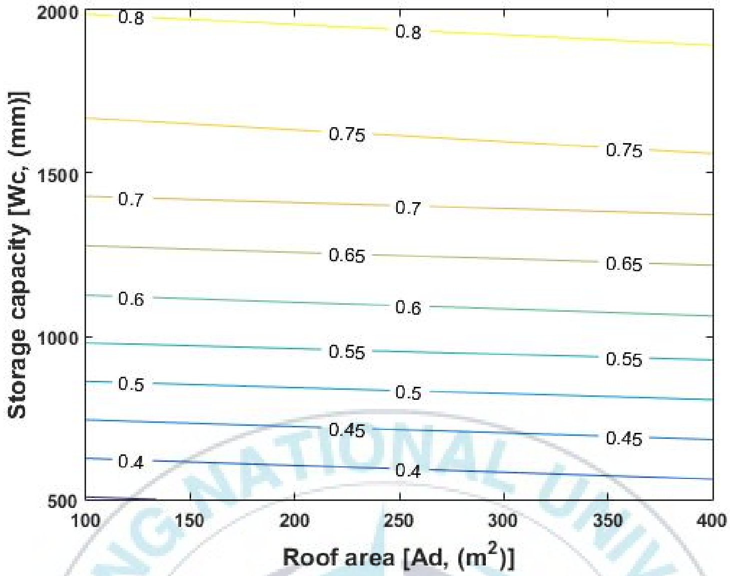

Fig. 3.14 Water supply reliability R_c varying with roof areas and storage capacities.

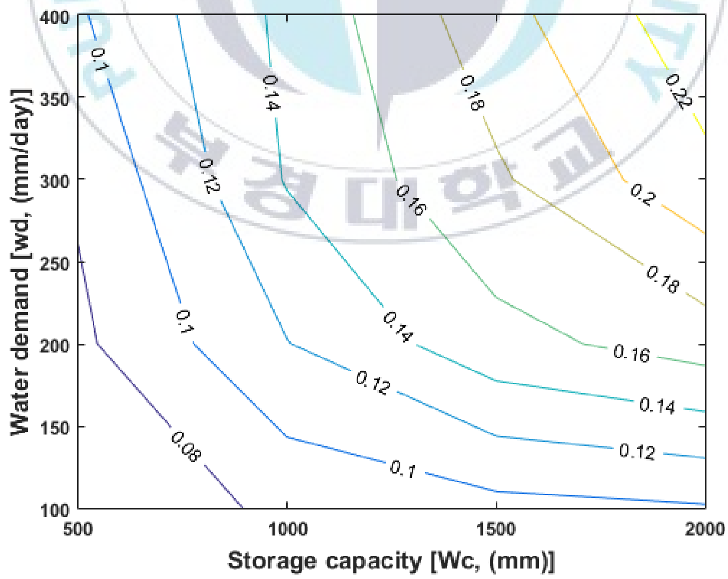

Fig. 3.15 Stormwater interception ratio R_r varying with storage capacities and water demands.

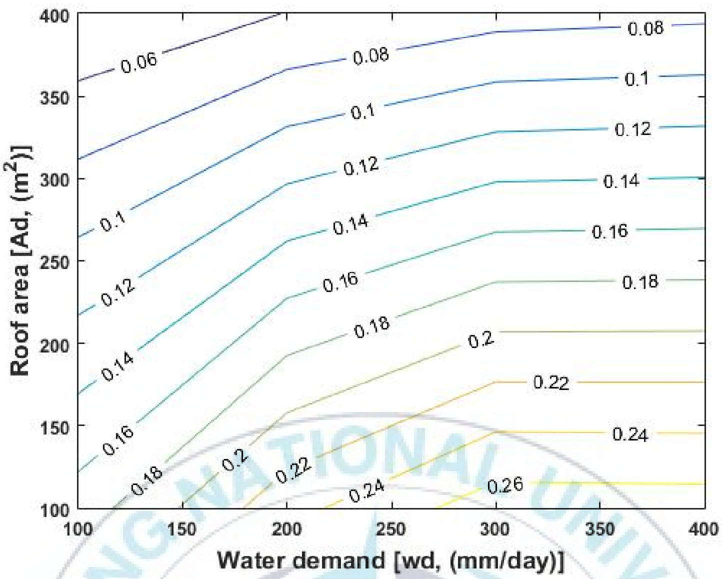

Fig. 3.16 Stormwater interception ratio R_r varying with water demands and roof areas.

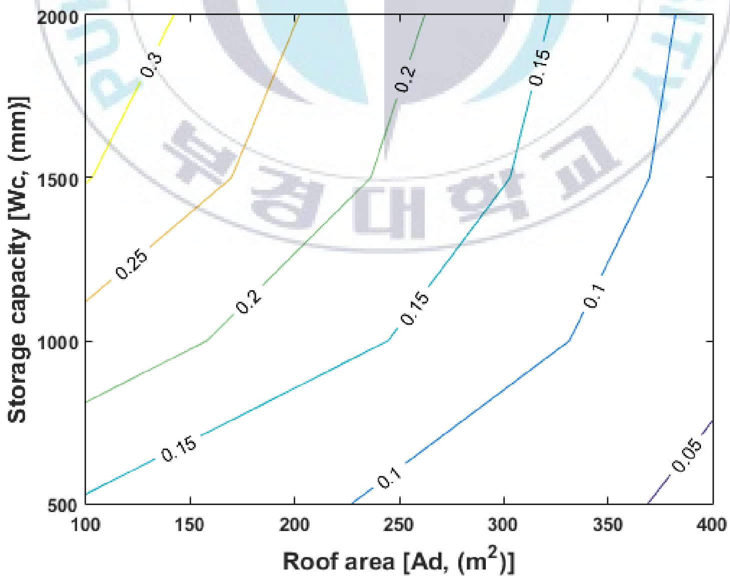

Fig. 3.17 Stormwater interception ratio R_r varying with roof areas and storage capacities.

Figs. 3.12–3.14 show the sensitivity of water supply reliability to RHS parameters. Increasing RHS capacity, decreasing water demand, and increasing catchment area can increase the reliability of water supply from RHS. Figs. 3.15–3.17 show the sensitivity of stormwater interception ratio to RHS parameters. Increasing RHS capacity, increasing water demand and decreasing catchment area have been shown to increase the efficiency of intercepting stormwater. As a result, using Figs. 3.12–3.17, the two parameters of RHS can easily be used to calculate the water supply reliability and stormwater interception ratio without going through the calculation process.

Also, the catchment area was found to be less sensitive to the performance of the RHS compared to the other two parameters, and it can be recognized that the capacity and water demand of the RHS mainly determine the performance of the RHS. In general, when RHS is applied to an existing building, the catchment area is often determined prior to the design of the RHS. Therefore, it would be reasonable to determine the capacity and water demand of the RHS to reflect the required water supply reliability and the required stormwater interception ratio. Alternatively, after determining the demand and capacity of the RHS corresponding to the required reliability, it may be possible to evaluate the ability to capture stormwater.

Ⅳ. Applications

4.1 Design formula of water supply reliability and stormwater interception ratio

In Chapter 3, the behavior of RHS according to the parameters was analyzed and the water supply reliability and stormwater interception ratio were estimated and shown. In this section, using the rainfall characteristics of the Busan site, a design formula for water supply reliability (R_e) and stormwater interception ratio (R_r) was derived using a combination of three RHS parameters (W_c, w_d and ϕ) as follows:

$$R_e = 0.00027286\,W_c - 0.0014282 w_d - 3.5366\phi + 0.6215 \quad (29)$$

$$R_r = 0.00007924\,W_c + 0.0002707 w_d + 27.177\phi - 0.1621 \quad (30)$$

Table 4.1 R^2 and RMSE between stochastic model and the estimated formula

	Water supply reliability (R_e)	Stormwater interception ratio (R_r)
R^2	0.9659	0.9104
RMSE	0.0328	0.0262

The design formula has the form of a multiple regression model ($f(W_c, w_d, \phi) = aW_c + bw_c + c\phi + d$), and the regression coefficients (a, b, c and d) are estimated using the least-squares method to best reproduce the outputs of the model proposed in this study. In order to evaluate the proposed design formulas, the design values obtained from the probabilistic model are compared with those of the corresponding design formulas (see Table 1). In addition, the design values of the probabilistic model and the design formula for the range of various parameters are compared and shown in Figs. 4.1-4.3.

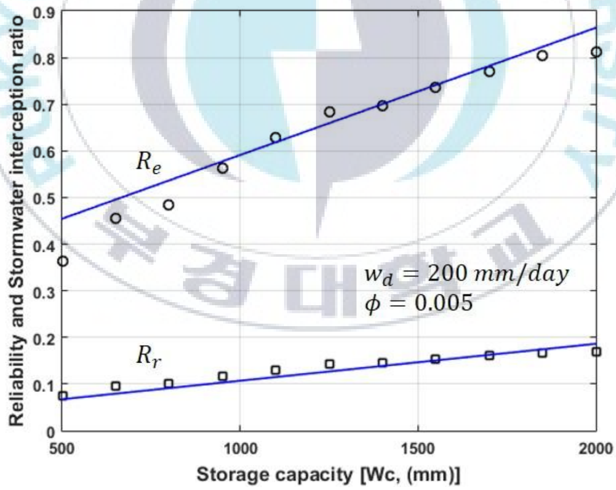

Fig. 4.1 Comparisons of water supply reliability and stormwater interception ratio of stochastic model and the estimated formula with varying storage capacities.

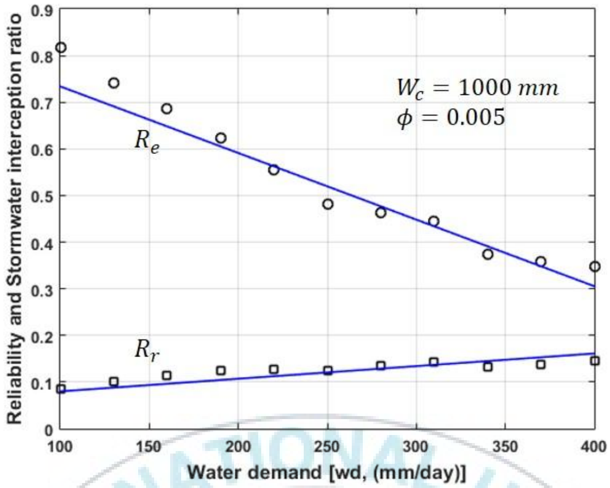

Fig. 4.2 Comparisons of water supply reliability and stormwater interception ratio of stochastic model and the estimated formula with varying water demands.

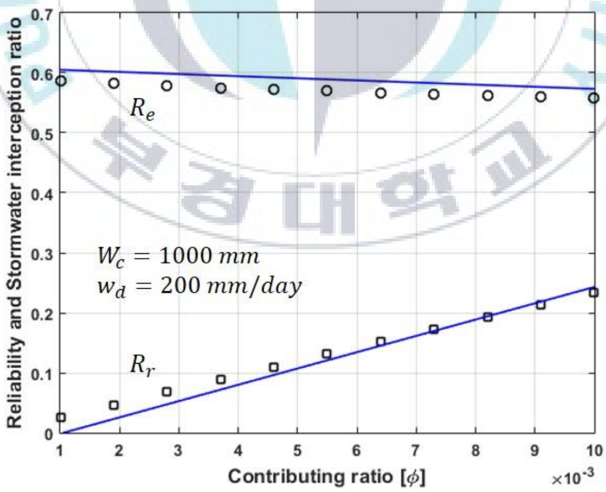

Fig. 4.3 Comparisons of water supply reliability and stormwater interception ratio of stochastic model and the estimated formula with varying contributing ratios.

Comparing R_e and R_r derived from the probabilistic model and the design formula, respectively, it is confirmed that R^2 is more than 0.9 and RMSE is satisfactorily small. The water supply reliability and stormwater interception ratio derived from the probabilistic model in Figs. 4.1-4.3 are indicated by ○ and □, respectively, and the corresponding values derived from the design formulas are indicated by solid blue lines. In terms of the agreement between the probabilistic model and the design formula for the various parameter ranges, the reliability of the design formula seems to be sufficiently secured. Therefore, it is expected that the proposed design formulas can be used to estimate the reliability of water supply and rainfall runoff in practical use, and can be fully utilized in RHS design.

4.2 RHS mitigates adverse effects of climate change

Climate model data have serious biases from observed data, and there are more biases in the results of rainfall simulations, especially since the simulation reliability for extreme weather events is relatively low (Boé et al., 2007). In order to use these data, the bias between the observed data and the model data should be corrected. In this study, Quantile-Mapping (QM) technique, which has been used in many studies and can be applied relatively easily, was used.

For more information see Kim et al. (2011), Seo et al. (2012), Sim et al. (2014), Lee et al. (2014), Choi et al. (2016), Lee et al. (2017), Cha et al. (2017), Lee et al. (2017), Cha et al. (2018), Kim et al. (2018), and Sim et al. (2019).

Before analyzing changes in stormwater due to climate change, climate model data were used to analyze how much annual precipitation changes in the future (see Fig. 4.4). In Fig. 4.4, 'present' is the range of ensemble of annual precipitation simulated under present (1981-2010) climate condition, while 'RCP 4.5' and 'RCP 8.5' represent the range of ensemble of annual precipitation simulated under future (2021-2050) climate conditions. Annual precipitation is likely to increase at Busan, Daegu, Daejeon, and Gwangju sites, while future annual precipitation is likely to decrease at Incheon and Seoul sites. It is projected that future annual precipitation under RCP 8.5 scenario will increase more than future annual precipitation under RCP 4.5 scenario, however the uncertainty in the RCP 8.5 scenario is greater than that in the RCP 4.5 scenario.

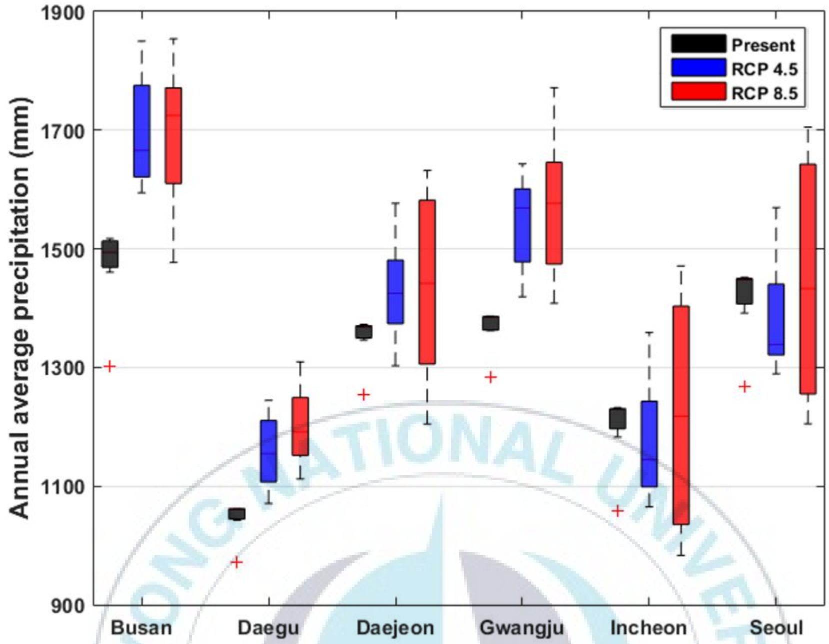

Fig. 4.4 Annual average precipitation of present and future climate data at 6 sites.

The parameters applied when analyzing the annual mean stormwater change due to climate change are: W_c = 1,000 mm, w_d = 200 mm/day, ϕ = 0.005. The annual average stormwater depths generated during the present and future periods without RHS and the annual average stormwater depths generated during the future period with RHS were estimated, respectively. These comparisons have shown how RHS can reduce stormwater increased by climate change (see Fig. 4.5). Looking at the Busan, Daegu, Daejeon, and Gwangju sites where the stormwater depth is likely to increase, we can find that the increased stormwater depth can be reduced almost by RHS. These results reveal that RHS can offset the adverse effects of climate change on stormwater management in cities.

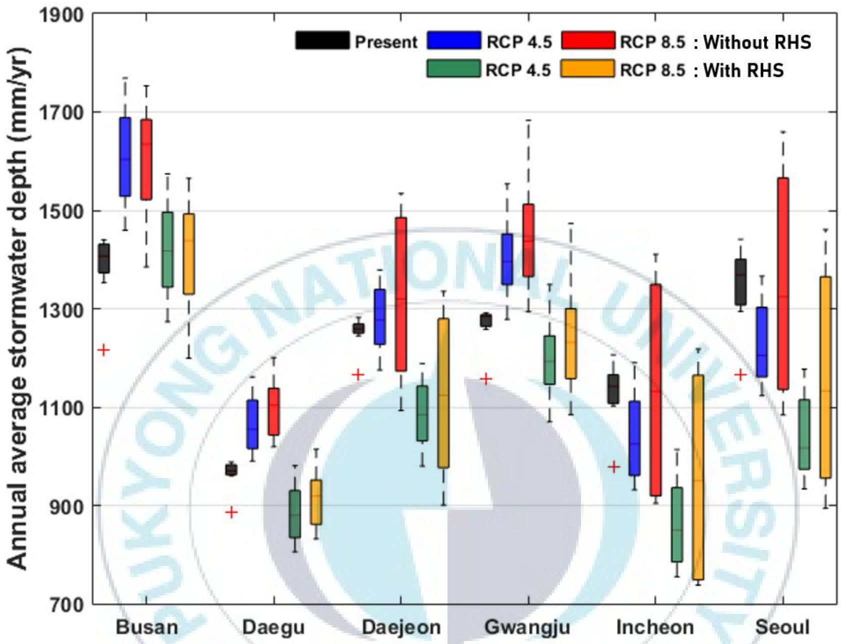

Fig. 4.5 Annual average stormwater depth of present and future climate data at 6 sites.

RHS has the ability to supply water stored in RHS as well as the ability to reduce stormwater increased by climate change. Fig. 4.6 shows the future water supply reliability achieved by RHS. Although site-specific, it can be found that the planned water supply plan from the RHS can be satisfied with about 50% confidence. Therefore, the introduction of RHS will provide additional benefits of securing available water resources as well as counteracting the adverse effects of climate change, such as stormwater reduction.

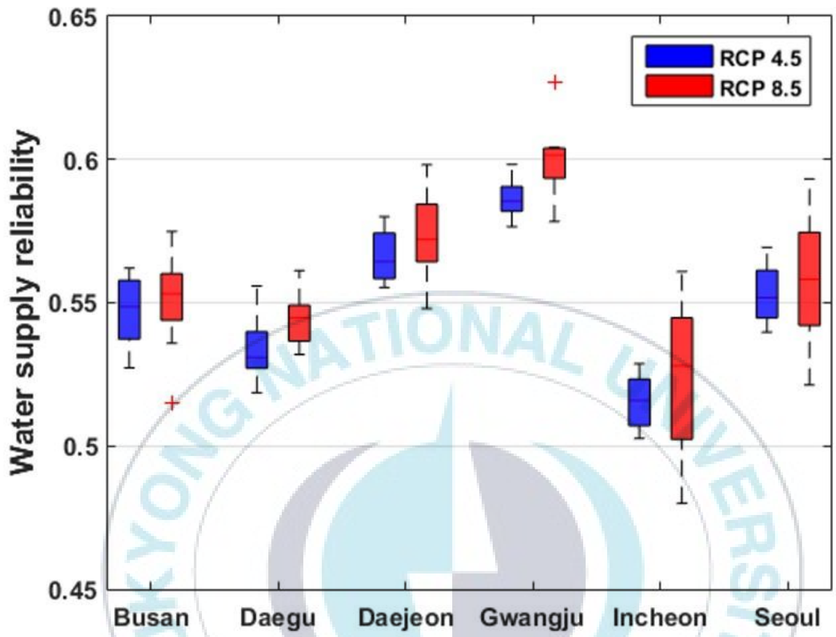

Fig. 4.6 Water supply reliability of future climate data at 6 sites.

Ⅴ. Conclusions

RHS is generally designed to collect and store rainwater falling on catchment surfaces (eg rooftops or other impervious areas) for home or urban multipurpose use (Choi et al., 2011). The performance of these RHSs is nonlinear with various factors such as climate, watershed characteristics, and RHS design specifications, so design optimization is necessary to balance cost and performance. The most commonly used indicators for RHS performance assessment are the water supply reliability from RHS and the stormwater interception efficiency expected from RHS (Keem et al., 2014). In this study, we focused on the stochastic characteristics of rainfall, and presented a probabilistic model for quantifying stormwater interception efficiency for stormwater management and reliability for water supply.

To verify the results of the derived probabilistic model, the results were compared with the numerical results. As a result of the comparison, it is confirmed that the numerical results and the results of the derived probabilistic model are in good agreement. We also analyzed the probabilistic behavior of RHS for changes in RHS characteristic parameters (capacity (W_c), water demand (w_d), and catchment area (A_d)). In the same rainfall event, increasing RHS capacity, decreasing water demand, and increasing catchment area were found to increase RHS water supply reliability. In addition, increased RHS capacity, increased water demand, and reduced catchment area were found to increase stormwater interception efficiency. In general, however, when RHS is actually applied to existing buildings, water demand and catchment area are often determined depending on the surrounding conditions. Therefore, the capacity of RHS will be the most important determinant of RHS behavior. In addition, design formulas for estimating water supply reliability and stormwater interception efficiency for characteristic parameters were derived so that they could be used in future RHS planning.

In this study, using various climate model data and proposed probability model, we investigated how much RHS can reduce future stormwater and how much water supply reliability can be obtained from RHS at 6 major sites in Korea. The RHS installation could play a role in responding to the possibility of future stormwater growth and additionally secure available water resources.

Using the probabilistic model proposed in this study, RHS water supply reliability and stormwater interception efficiency can be easily implemented in relatively simple computer codes. Therefore, the results of this study are expected to be useful tools for evaluating RHS performance, determining RHS capacity, and analyzing the role of RHS as a means of adaptation to climate change. Overall, this probabilistic approach has proven to be feasible and reliable in modeling the long-term balance of RHS. The proposed solution needs to emphasize that the daily precipitation series is valid for RHS located in areas that can be approximated by exponential distribution.

In addition, this study is the result of applying to the probabilistic model using the values of general parameters, not the analysis applied to actual buildings. For further study, it would be good to analyze the effect of RHS in actual buildings. Through this, after the RHS is installed in the actual building, the climate change scenario is applied to examine the impact on climate change of the city, and then the water supply reliability and stormwater interception ratio are calculated. Therefore, it would be good to analyze the available water resources and future stormwater reduction in the entire city.

As a result, the derived model can easily estimate the water supply reliability and stormwater interception ratio using only the rainfall parameter and the RHS characteristic parameter, and if rainfall data by site is inputted, the rainfall characteristic parameters can be applied to estimate water supply reliability and stormwater capture efficiency according to various climates. In addition, multiple regression equations can be used to evaluate water supply reliability and stormwater capture efficiency based on the parameters of the RHS facility, making it easier to evaluate the performance of the facility. Therefore, the probabilistic model is meaningful in that it provides an easy-to-use tool for high accuracy and wider coverage of the facility's performance for the installation plan and design of the LID in the context of increased interest and installation of the LID facility. In the future, the results of this study can easily estimate the water supply reliability and stormwater interception ratio and can be used in the RHS installation planning. In addition, like the probabilistic model derived in this study, the probabilistic model can be derived for other LID facilities besides RHS.

References

Ahiablame, L. M., Engel, B. A. and Chaubey, I. (2013). Effectiveness of low impact development practices in two urbanized watersheds: Retrofitting with rain barrel/cistern and porous pavement. Journal of environmental management, 119, p. 151-161.

Baek, J., Kim, H., Shin, H., Kim, J. and Park, K. (2018). A study on the optimum size of rainwater utilization in detached residential complex. Journal of Korean Society on Water Environmental, 34(6), p. 669-677.

Basinger, M., Montalto, F. and Lall, U. (2010). A rainwater harvesting system reliability model based on nonparametric stochastic rainfall generator. Journal of Hydrology, 392(3-4), p. 105-118.

Becciu, G., Raimondi, A. and Dresti, C. (2018). Semi-probabilistic design of rainwater tanks: a case study in Northern Italy. Urban Water Journal, 15(3), p. 192-199.

Boé, J., Terray, L., Habets, F. and Martin, E. (2007). Statistical and dynamical downscaling of the Seine basin climate for hydro-meteorological studies. International Journal of Climatology: A Journal of the Royal Meteorological Society, 27(12), p. 1643-1655.

Butler, D., Memon, A., Makropoulos, C., Southall, A. and Clarke, L. (2010). Guidance on water cycle management for new developments. CIRIA Report C690.

Campisano, A., Butler, D., Ward, S., Burns, M. J., Friedler, E., DeBusk, K., Fisher-Jeffes, L. N., Ghisi, E., Rahman, A., Furumai, H. and Han, M. (2017). Urban rainwater harvesting systems: Research, implementation and future perspectives. Water Research, 115, p. 195-209.

Cha, W., Lee, O., Choi, J., Lee, J. and Kim, S. (2018). Future hourly rainfall data production using point rainfall model and future stormwater analysis. Journal of the Korean Society of Hazard Mitigation, 18(2), p. 483-492.

Cha, W., Lee, O., Kim, S. and Park, Y. (2017). Analysis of indicators of hydrological alteration on the Geumho river basin under AR5 RCP scenarios. Journal of the Korean Society of Hazard Mitigation, 17(4), p. 317-326.

Chang, J. S. and, Cooper, G. (1970). A practical difference scheme for Fokker-Planck equations. Journal of Computational Physics, 6(1), p. 1 - 16.

Che-Ani, A. I., Shaari, N., Sairi, A., Zain, M. F. M. and Tahir, M. M. (2009). Rainwater harvesting as an alternative water supply in the future. European Journal of Scientific Research, 34(1), p. 132-140.

Choi, C. H., Park, M. J., Baek, C. W. and Kim, S. (2011). Application of rainwater harvesting system reliability model based on non-parametric stochastic daily rainfall generator to Haundae district of Busan. Journal of Korean Society on Water Quality, 27(5), p. 634-645.

Choi, J., Lee, O. and Kim, S. (2016). Analysis of the effect of climate change on IDF curves using scale-invariance technique: Focus on RCP 8.5. Journal of Korea Water Resources Association, 49(12), p. 995-1006.

Chui, T. F. M., Liu, X. and Zhan, W. (2016). Assessing cost-effectiveness of specific LID practice designs in response to large storm events. Journal of hydrology, 533, p. 353-364.

Cowden, J. R., Watkins Jr, D. W. and Mihelcic, J. R. (2008). Stochastic rainfall modeling in West Africa: Parsimonious approaches for domestic rainwater harvesting assessment. Journal of Hydrology, 361(1-2), p. 64-77.

Eckart, K., McPhee, Z. and Bolisetti, T. (2018). Multiobjective optimization of low impact development stormwater controls.

Journal of hydrology, 562, p. 564-576.

Eroksuz, E. and Rahman, A. (2010). Rainwater tanks in multi-unit buildings: A case study for three Australian cities. Resources, Conservation and Recycling, 54(12), p. 1449-1452.

Ghisi, E. (2006). Potential for potable water savings by using rainwater in the residential sector of Brazil. Building and Environment, 41(11), p. 1544-1550.

Guo, R. and Guo, Y. (2018). Stochastic modelling of the hydrologic operation of rainwater harvesting systems. Journal of hydrology, 562, p. 30-39.

Guo, R., Guo, Y. and Wang, J. (2018). Stormwater capture and antecedent moisture characteristics of permeable pavements. Hydrological processes, 32(17), p. 2708-2720.

Guo, Y. and Baetz, B. W. (2007). Sizing of rainwater storage units for green building applications. Journal of Hydrologic Engineering, 12(2), p. 197-205.

Guo, Y. and Gao, T. (2016). Analytical equations for estimating the total runoff reduction efficiency of infiltration trenches. Journal of Sustainable Water in the Built Environment, 2(3), 06016001.

Guo, Y., Zhang, S. and Liu, S. (2014). Runoff reduction capabilities and irrigation requirements of green roofs. Water resources management, 28(5), p. 1363-1378.

Han, M. (2002). Overseas rainwater use case. Planning and Policy, p. 62-68.

Hong, W. H., Bae, S. H. and Choi, M. Y. (2005). A Study on the Economic Evaluation by Introducing Facility to Use Rainwater in Daegu Worldcup Stadium. Journal of the Architectural Institute of Korea Planning & Design, 21(8), p. 243-250.

Jennings, A. A., Adeel, A. A., Hopkins, A., Litofsky, A. L. and Wellstead, S. W. (2012). Rain barrel-urban garden stormwater management performance. Journal of Environmental Engineering,

139(5), p. 757-765.
Kang, T., Koo, Y. and Lee, S. (2015). A study on design method and effect analysis of rainwater harvesting facility for efficient use. Journal of the Korean Society of Hazard Mitigation, 15(2), p. 353-361.
Kahinda, J. M. M., Taigbenu, A. E. and Boroto, J. R. (2007). Domestic rainwater harvesting to improve water supply in rural South Africa. Physics and Chemistry of the Earth, Parts A/B/C 32(15-18), p. 1050-1057.
Kavvas, M. L. (2003). Nonlinear hydrologic processes: Conservation equations for determining their means and probability distributions. Journal of Hydrologic Engineering, 8(2), p. 44-53.
Keem, M., Kang, D., Park, M. and Kim, S. (2014). Parameter estimation methods of rainwater harvesting system reliability model for improving the applicability to Korea: Application to Busan, Korea. Journal of the Korean Society of Hazard Mitigation, 14(2), p. 345-354.
Kim, E., Choi, H. I., Park, M. J., Cho, S. J. and Kim, S. (2011). The effect of climate change on Korean drought occurrences using a stochastic soil water balance model. Scientific Research and Essays, 6(13), p. 2771-2783.
Kim, H., Han, M. and Lee, J. Y. (2012). The application of an analytical probabilistic model for estimating the rainfall - runoff reductions achieved using a rainwater harvesting system. Science of the total environment, 424, p. 213-218.
Kim, H. J., Jang, C. H. and Noh, S. J. (2012). Development and application of the catchment hydrologic cycle assessment tool considering urbanization (I)-Model development. Journal of Korea Water Resources Association, 45(2), p. 203-215.
Kim, K., Lee, J., Keum, J., Park, M. and Kim, S. (2018). Uncertainty of future intensity-duration-frequency curves using multi-regional

climate models. Journal of the Korean Society of Hazard Mitigation, 18(6), p. 405-416.

Kim, K., Park, H., Kim, T. and Han, M. (2014). Evaluation of stored rainwater quality and economic efficiency at Yangdo elementary rainwater harvesting system. Journal of Korean Society of Environmental Engineers, 36(5), p. 333-341.

Kim, K., Yoo, C. and Yun, Z. (2008). Hydrological evaluation of rainwater harvesting: 2. Hydrological evaluation. Journal of Korean Society on Water Quality, 24(2), p. 230-238.

Kim, S. and Han, S. (2010). Urban Stormwater Capture Curve Using Three-Parameter Mixed Exponential Probability Density Function and NRCS Runoff Curve Number Method. Water Environment Research, 82(1), p. 43-50.

Kim, S., Han, S. and Kim, E. (2011). Stochastic modeling of soil water and plant water stress using cumulant expansion theory. Ecohydrology, 4(1), p. 94-105.

Lee, A., Cho, S., Kang, D. K. and Kim, S. (2014). Analysis of the effect of climate change on the Nakdong river stream flow using indicators of hydrological alteration. Journal of hydro-environment research, 8(3), p. 234-247.

Lee, O., Jang, J., Park, M. J., Lee, Y. and Kim, S. (2017). Estimation of PMP in nuclear power plants area considering climate change. Journal of the Korean Society of Hazard Mitigation, 17(6), p. 549-557.

Lee, O., Jo, D. J. and Kim, S. (2017). Future PMP estimation of Chungjudam watershed under KMA climate change scenarios. Journal of the Korean Society of Hazard Mitigation, 17(1), p. 365-373.

Lee, S. (2004). Environment-Friendly Rainwater Utilization Status in Germany. Planning and Policy, p. 96-101.

Mao, X., Jia, H. and Shaw, L. Y. (2017). Assessing the ecological benefits of aggregate LID-BMPs through modelling. Ecological modelling, 353, p. 139-149.

Menció, A. and Mas-Pla, J. (2008). Assessment by multivariate analysis of groundwater-surface water interactions in urbanized Mediterranean streams. Journal of hydrology, 352(3-4), p. 355-366.

Okoye, C. O., Solyalı, O. and Akıntuğ, B. (2015). Optimal sizing of storage tanks in domestic rainwater harvesting systems: A linear programming approach. Resources, Conservation and Recycling, 104, p. 131-140.

Palla, A., Gnecco, I. and Lanza, L. G. (2011). Non-dimensional design parameters and performance assessment of rainwater harvesting systems. Journal of Hydrology, 401(1-2), p. 65-76.

Palla, A., Gnecco, I., Lanza, L. G. and La Barbera, P. (2012). Performance analysis of domestic rainwater harvesting systems under various European climate zones. Resources, Conservation and Recycling, 62, p. 71-80.

Park, J. W. and Cho, Y. S. (2015). Establishing Indicators and Stream Depletion Potential Index (SDPI) for Stream Health. J. Korean Soc. Hazard Mitig, 15(2), p. 285-292.

Park, S., Kim, S. and Kwak, D. (2007). An analysis of rainwater quality in rainwater harvesting system at domitories in Seoul nation university, Seoul, Korea. Journal of Society of Rain Masters, 1(1), p. 96-102.

Sample, D. J. and Liu, J. (2014). Optimizing rainwater harvesting systems for the dual purposes of water supply and runoff capture. Journal of Cleaner Production, 75, p. 174-194.

Seo, L., Jeon, M., Kim, T. W. and Kim, S. (2012). Ensemble prediction of future design rainfalls considering climate change. Journal of the Korean Society of Hazard Mitigation, 12(2), p. 159-172.

Shuster, W. D., Bonta, J., Thurston, H., Warnemuende, E. and Smith, D. R. (2005). Impacts of impervious surface on watershed hydrology:

A review. Urban Water Journal, 2(4), p. 263-275.
Sim, H. J., Ahn, M. and Kim, S. (2014). Feasibility assessment of RCP 8.5 in extreme air temperature. Journal of the Korean Society of Hazard Mitigation, 14(3), p. 351-359.
Sim, I., Lee, O. and Kim, S. (2019). Sensitivity Analysis of Extreme Daily Rainfall Depth in Summer Season on Surface Air Temperature and Dew-Point Temperature. Water, 11(4), p. 771.
Su, M. D., Lin, C. H., Chang, L. F., Kang, J. L. and Lin, M. C. (2009). A probabilistic approach to rainwater harvesting systems design and evaluation. Resources, Conservation and Recycling, 53(7), p. 393-399.
Thomas, T. (1998). Domestic water supply using rainwater harvesting. Building Research & Information, 26(2), p. 94-101.
Ward, S., Memon, F. A. and Butler, D. (2012). Performance of a large building rainwater harvesting system. Water research, 46(16), p. 5127-5134.
Yoo, C., Kim, K. and Yun, Z. (2008). Hydrological evaluation of rainwater harvesting: 1. Hydrological analysis, Journal of Korean Society on Water Quality, 24(2), p. 221-229.
Zaizen, M., Urakawa, T., Matsumoto, Y. and Takai, H. (2000). The collection of rainwater from dome stadiums in Japan. Urban water, 1(4), p. 355-359.
Zhang, G., Hamlett, J. M., Reed, P. and Tang, Y. (2013). Multi-objective optimization of low impact development designs in an urbanizing watershed. Open Journal of Optimization, 2(04), p. 95.
Zhang, S. and Guo, Y. (2012a). Analytical probabilistic model for evaluating the hydrologic performance of green roofs. Journal of Hydrologic Engineering, 18(1), p. 19-28.
Zhang, S. and Guo, Y. (2012b). Explicit equation for estimating storm-water capture efficiency of rain gardens. Journal of Hydrologic Engineering, 18(12), p. 1739-1748.

Zhang, S. and Guo, Y. (2014a). Analytical equation for estimating the stormwater capture efficiency of permeable pavement systems. Journal of Irrigation and Drainage Engineering, 141(4), 06014004.
Zhang, S. and Guo, Y. (2014b). Stormwater capture efficiency of bioretention systems. Water resources management, 28(1), p. 149-168.